

Characterization of an agostic bond on the basis of the electron density

P.L.A. Popelier *, G. Logothetis

Department of Chemistry, U.M.I.S.T., 88 Sackville Street, Manchester M60 1QD, UK

Received 13 October 1997

Abstract

Several conformations of $\text{CH}_3\text{TiCl}_2^+$, $\text{C}_2\text{H}_5\text{TiCl}_2^+$ and $\text{C}_3\text{H}_7\text{TiCl}_2^+$ were selected for a case study on agostic bonds. Ab initio wavefunctions have been generated at Hartree–Fock, BLYP and MP2 level. Criteria solely based on a topological analysis of the electron density are proposed in order to characterize the agostic bond. These criteria are drawn from the theory of ‘atoms in molecules’ (AIM) and form an independent complement to conventional methods like IR, NMR and structural crystallography. The observed features systematically violate the criteria that have been proposed for hydrogen bonding. As a consequence the agostic bond is not a special type of hydrogen bond. © 1998 Elsevier Science S.A. All rights reserved.

Keywords: Ab initio; Agostic; Ti–alkyl; Charge density; Topological analysis

1. Introduction

In the chemical literature a great deal of attention is devoted to the understanding of special interactions between specific atoms in a molecule. Indeed chemistry would be severely restricted and impoverished if a molecule were a mere conglomerate of atoms held together by virtue of a reduced total (molecular) energy. Quite to the contrary one of the most successful schemes to rationalize molecular stability and patterns is the chemical bond, which is a chief example of a special interaction between a pair of atoms. But sometimes it is not clear which atom is bonded to which other and to what degree, if at all, if one resorts to a simple model like Lewis structures. For such cases a more modern theory is warranted that enables one to extract chemical bonds from computed wavefunctions. A prime candidate theory to fulfill that purpose is the theory of ‘atoms in molecules’ (AIM) [1,2]. It unambiguously defines what a bond is and should therefore be considered as an excellent instrument to study agostic bonds as we will show in this contribution.

Already in the sixties—before the agostic interaction was given its name—it was found that some C–H bonds of transition metal ligands were orientated in a manner indicating some weak interaction between the metal and the hydrogen [3]. Trofimenko was one of the first to observe unusual low fields shifts for ethyl hydrogens in the ^1H -NMR spectrum of a Ni–boron complex [4] and suggested that the hydrogens were held close to the nickel centre. Subsequently spectroscopically determined C–H bond lengthening (reduced C–H stretching frequencies) in a Mo complex supported the hypothesis of a special C–H...M interaction [5]. Cotton proposed a C...H...Mo three-center-two-electron bond appearing in this complex based on a X-ray diffraction study yielding the remarkably short H...Mo distance of 2.2 Å [6]. More compelling evidence for such an unusually short H...M distance had to await the first neutron diffraction study on an Fe complex which definitely showed the position of the agostic hydrogen [7]. Finally the

* Corresponding author. Tel.: +44 161 2004511; fax: +44 151 2367677; e-mail: pla@umist.ac.uk

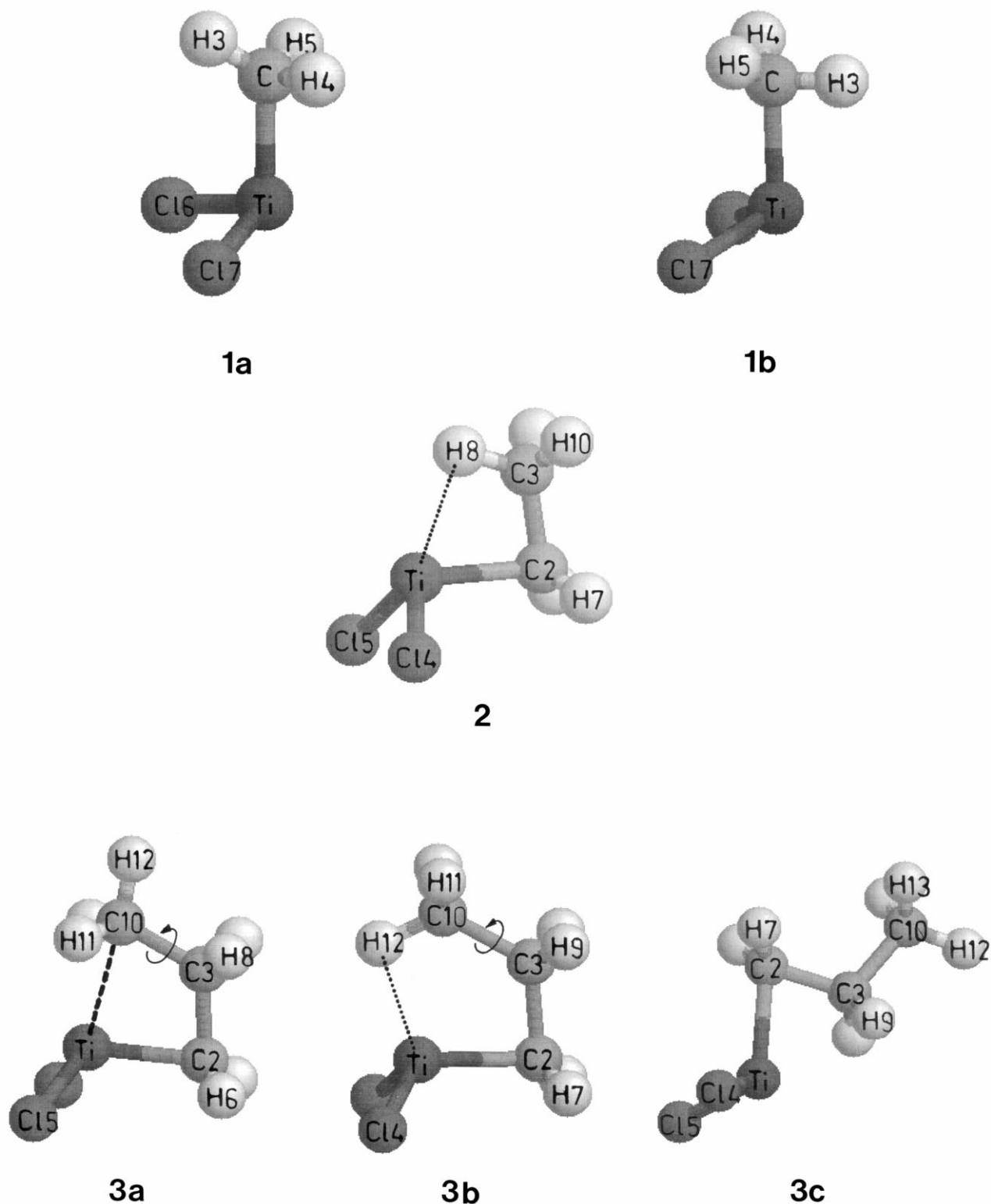


Fig. 1. Numbering scheme for two conformations of $\text{CH}_3\text{TiCl}_2^+$ (**1a**, **1b**), $\text{C}_2\text{H}_5\text{TiCl}_2^+$ (**2**) and three structures of $\text{C}_3\text{H}_7\text{TiCl}_2^+$ (**3a**, **3b**, **3c**). The two agostic bonds are marked by dotted lines and the dashed line in **3a** denotes the Ti–C bond which is ruptured upon rotation of the terminal methyl group around the $\text{C}_3\text{--C}_{10}$ bond.

consistent anomalies observed in IR, NMR and crystallographic study pointing towards a commonly appearing C–H–M bond lead Brookhart and Green to

reserve a special name for this interaction. The name ‘agostic’ was introduced in their 1983 review [8] and has since been widely accepted.

Table 1
Selected geometrical parameters (Å and °) and energies (a.u.) of CH₃TiCl₂⁺ (**1a**) and (**1b**), both molecules contain a mirror plane (Cs)

| | HF (1a) | BLYP (1a) | MP2 (1a) | HF(1b) | BLYP(1b) | MP2(1b) |
|-------------------------------------|------------------|--------------------|-------------------|-----------------|-------------------|------------------|
| Ti–C | 1.9670 | 1.9906 | 1.9675 | 1.9670 | 1.9948 | 1.9789 |
| Ti–Cl | 2.1143 | 2.1351 | 2.1040 | 2.1137 | 2.1346 | 2.1038 |
| C–H ₃ | 1.0819 | 1.0990 | 1.0855 | 1.1030 | 1.1252 | 1.1183 |
| C–H ₄ | 1.0926 | 1.1122 | 1.1056 | 1.0825 | 1.0996 | 1.0890 |
| H ₃ –C–Ti | 117.25 | 123.11 | 132.16 | 94.50 | 89.88 | 88.09 |
| H ₄ –C–Ti | 101.51 | 99.85 | 97.00 | 112.82 | 116.06 | 118.69 |
| Cl ₆ –Ti–Cl ₇ | 115.21 | 109.30 | 107.88 | 115.31 | 109.30 | 108.08 |
| Cl–Ti–C | 102.90 | 103.27 | 103.52 | 105.15 | 105.07 | 105.42 |
| H ₃ –C–H ₄ | 111.59 | 110.59 | 109.59 | 111.45 | 110.31 | 108.59 |
| H ₄ –C–H ₅ | 112.73 | 112.12 | 109.73 | 112.56 | 111.98 | 110.82 |
| H ₃ –C–Ti–Cl | 60.0 | 56.9 | 56.3 | 118.9 | 122.4 | 122.9 |
| H ₄ –C–Ti–Cl | 178.2 | –179.6 | 179.2 | 125.6 | 125.0 | 126.9 |
| Energy | –1806.48333 | –1809.31079 | –1807.00712 | –1806.48254 | –1809.30978 | –1807.00627 |

In summary, the existence of C–H–M bridges can be deduced from four criteria [9]: crystallographic data, NMR chemical shifts to high field ($\delta = -5$ to -15 ppm), reduced NMR coupling constants ($^1J(\text{C,H}) = 75\text{--}100$ MHz) and low vibrational frequencies ($\nu_{\text{CH}} = 2700\text{--}2300$ cm⁻¹). In this paper we propose an entirely independent fifth criterion to detect and study agostic interaction. Our collection of criteria is drawn from the theory of AIM and requires an accurate charge density which is of computational origin in our case. It should be emphasized that the AIM properties only require the knowledge of a molecule's charge density which can also be experimentally determined [10].

As an example to illustrate the use of AIM in the context of agostic interactions we have chosen the well-known TiCl₂–alkyl complexes. The results presented here may improve the understanding of transition metal catalysis, in particular in Ziegler–Natta

polymerization. Inspired by earlier theoretical work we have systematically studied several conformations of CH₃TiCl₂⁺, C₂H₅TiCl₂⁺ [11,12] which will be discussed in subsequent sections but first we comprehensively review a few necessary AIM concepts.

2. How to define a bond

For diatomics it is straightforward to determine whether the two atoms are bonded or not: if there is a finite internuclear separation r_0 for which the diatomic's energy $E(r_0)$ is a minimum then there is a bond between the two atoms. It is not at all straightforward how this definition can be extended to a polyatomic molecule. Suppose that the energy of a polyatomic is known as a function of its nuclear coordinates how can one then assign which atoms are bonded to which? Given that the total system of atoms (i.e. the molecule) is bound how can one single out special pairs of atoms and call them bonded?

AIM's answer is based on the concept of a gradient path which is a curve such that the gradient vector $\nabla\rho$ is tangent to it in every point (except where $\nabla\rho = \mathbf{0}$). It is helpful to view the gradient path as a sequence of infinitesimal gradient vectors—the next one evaluated at the end point of the current one. Because gradient vectors have a sense gradient paths also have a sense, i.e. they point in the direction of higher charge density. There is a special gradient path which originates at the so-called bond critical point (BCP) and terminates at a nucleus. Critical points (CP) are extrema in the charge density or points in space where $\nabla\rho$ vanishes. The two gradient paths each starting at the BCP and terminating at a nucleus are called the atomic interaction line. If all forces on all the nuclei vanish the atomic interaction line becomes a bond path (BP). Practically this is a line linking two nuclei which we consequently call bonded. So the necessary and sufficient condition for two atoms

Table 2
Selected geometrical parameters (Å and °) and energies (a.u.) of C₂H₅TiCl₂⁺ (**2**), this molecule contains a mirror plane (Cs)

| | HF | BLYP | MP2 |
|---|--------------|--------------|--------------|
| Ti–C | 1.9881 | 2.0172 | 1.9963 |
| Ti–Cl | 2.1303 | 2.1418 | 2.1071 |
| Ti–H ₈ | 2.0706 | 2.0660 | 2.0286 |
| C–C | 1.5107 | 1.5350 | 1.5354 |
| C ₂ –H ₇ | 1.0805 | 1.0982 | 1.0877 |
| C ₃ –H ₈ | 1.1279 | 1.1447 | 1.1284 |
| C ₃ –H ₁₀ | 1.0809 | 1.0989 | 1.0864 |
| Ti–C ₂ –C ₃ | 86.68 | 84.85 | 83.31 |
| Cl ₄ –Ti–C ₂ | 104.50 | 105.86 | 105.66 |
| Cl ₄ –Ti–Cl ₅ | 119.00 | 112.21 | 110.69 |
| Ti–C ₂ –H ₇ | 110.36 | 112.85 | 115.86 |
| C ₂ –C ₃ –H ₈ | 113.24 | 114.35 | 115.32 |
| C ₂ –C ₃ –H ₁₀ | 112.90 | 112.84 | 112.48 |
| Ti–H ₈ –C ₃ | 94.02 | 93.53 | 93.01 |
| Ti–C–H ₉ | 116.3 | 116.5 | 117.1 |
| Cl ₄ –Ti–C–C | 117.1 | 120.4 | 121.3 |
| Energy | –1845.542176 | –1848.618438 | –1846.207070 |

Table 3

Selected geometrical parameters (Å and °) and energies (a.u.) of C₃H₇TiCl₂⁺ (**3a**), (**3b**) and (**3c**), all molecules contain a mirror plane (Cs)

| | HF (3a) | BLYP (3a) | MP2 (3a) | HF(3b) | BLYP(3b) | MP2(3b) | HF(3c) | BLYP(3c) | MP2(3c) |
|---|------------------|--------------------|-------------------|-----------------|-------------------|------------------|-----------------|-------------------|------------------|
| Ti–H ₁₂ | — | — | — | 1.9394 | 1.9072 | 1.8831 | — | — | — |
| Ti–C ₁₀ | 2.2665 | 2.2249 | 2.2078 | 2.3650 | 2.3287 | 2.2994 | — | — | — |
| Ti–C ₂ | 1.9621 | 2.0001 | 1.9855 | 1.9387 | 1.9832 | 1.9694 | 1.9694 | 1.9985 | 1.9825 |
| Ti–Cl _{4/5} ^a | 2.1410 | 2.1503 | 2.1159 | 2.1372 | 2.1474 | 2.1147 | 2.1396 | 2.1470 | 2.1125 |
| Ti–C ₁₀ | 2.2665 | 2.2249 | 2.2078 | 2.3650 | 2.3287 | 2.2994 | 3.8272 | 3.8277 | 3.7408 |
| C ₃ –C ₁₀ | 1.5884 | 1.6089 | 1.5825 | 1.6156 | 1.6297 | 1.6030 | 1.5513 | 1.5598 | 1.5317 |
| C ₂ –C ₃ | 1.5422 | 1.5658 | 1.5608 | 1.5554 | 1.5791 | 1.5816 | 1.5250 | 1.5600 | 1.5588 |
| C ₂ –H _{6/7} | 1.0806 | 1.0976 | 1.0878 | 1.0805 | 1.0976 | 1.0874 | 1.0801 | 1.0979 | 1.0881 |
| C ₃ –H _{8/9} | 1.0800 | 1.0978 | 1.0864 | 1.0784 | 1.0963 | 1.0847 | 1.1010 | 1.1208 | 1.1105 |
| C ₁₀ –H _{11/13} | 1.1010 | 1.1201 | 1.1080 | 1.0799 | 1.0981 | 1.0868 | 1.0809 | 1.0983 | 1.0866 |
| C ₁₀ –H ₁₂ | 1.0799 | 1.0990 | 1.0865 | 1.1173 | 1.1452 | 1.1286 | 1.0810 | 1.0993 | 1.0876 |
| C ₁₀ –Ti–C ₂ | 78.02 | 80.19 | 80.35 | — | — | — | — | — | — |
| C ₁₀ –H ₁₂ –Ti | — | — | — | 97.74 | 96.23 | 96.31 | — | — | — |
| Cl ₄ –Ti–C ₂ | 104.95 | 107.09 | 106.36 | 106.76 | 108.85 | 109.11 | 104.76 | 106.58 | 106.61 |
| Cl ₄ –Ti–Cl ₅ | 119.24 | 113.89 | 112.51 | 120.61 | 115.03 | 113.90 | 118.94 | 112.95 | 111.67 |
| Ti–C ₂ –C ₃ | 88.00 | 84.80 | 84.07 | 85.79 | 83.14 | 81.61 | 80.76 | 78.44 | 76.42 |
| C ₂ –C ₃ –C ₁₀ | 117.19 | 118.38 | 119.16 | 123.01 | 123.70 | 124.86 | 112.24 | 113.26 | 112.71 |
| Ti–C ₁₀ –C ₃ | 76.80 | 76.63 | 76.42 | — | — | — | — | — | — |
| H _{11/13} –C ₁₀ –C ₃ | 115.35 | 115.39 | 115.20 | 108.66 | 109.13 | 109.23 | 109.84 | 109.79 | 109.57 |
| H ₁₂ –C ₁₀ –C ₃ | 107.12 | 107.83 | 108.04 | 125.50 | 126.07 | 125.61 | 109.14 | 109.51 | 110.11 |
| Cl ₄ –Ti–C ₂ –C ₃ | 116.8 | 118.7 | 119.9 | 114.9 | 117.0 | 117.5 | 117.0 | 119.6 | 120.3 |
| H _{11/13} –C ₁₀ –C ₃ –C ₂ | 66.1 | 65.7 | 65.6 | –120.7 | –120.4 | –120.4 | –60.2 | –60.0 | –59.8 |

^a The slash signifies that a symmetry related (mirror plane) atom follows. This facilitates the correspondence with the numbering scheme of Fig. 1.

to be bonded is the presence of a bond path between them. This definition is valid for any polyatomic and rigorously enables the interpretation of a molecule as a set of bonded atoms. This is one of the cornerstones of AIM and will be taken advantage of in this work.

3. How to define an atomic property

Another cornerstone of the theory of AIM is the definition of an atom which is important in this work to define for example the population (and thus the net charge) of an atom. The theory of AIM is often thought of as yet another method to define atomic populations. This is a false assumption for the atomic population according to AIM is just a by-product of the theory. In fact AIM offers a more profound insight into the chemistry of a molecule than other ad hoc methods which have been especially designed just to compute atomic populations.

Table 4

Energies (a.u.) of C₃H₇TiCl₂⁺ (**3a**), (**3b**) and (**3c**)

| | HF | BLYP | MP2 |
|-----------|--------------|--------------|--------------|
| 3a | –1884.592140 | –1887.923363 | –1885.406706 |
| 3b | –1884.580969 | –1887.915389 | –1885.397565 |
| 3c | –1884.588070 | –1887.914401 | –1885.399796 |

Most gradient paths terminate at a nucleus. The collection of gradient paths that each nucleus attracts is called an atomic basin, denoted by Ω , which constitutes the portion of space allocated to an atom. It is over this volume that properties are integrated to yield atomic properties, for example the integration of ρ yields the atom's population. It is also possible to define the atom's dipolar polarization $M(\Omega)$ which measures the displacement of the atom's centroid of negative charge from the position of the nucleus. Perhaps the most remarkable atomic property is the atom's energy $E(\Omega)$. Its existence is justified because an atom obeys the virial theorem—a most important theorem which is also obeyed by the total system or the molecule.

In summary, AIM studies the topology of the charge density which is revealed by computing $\nabla\rho$. The gradient of ρ gives rise to gradient paths which slice the charge density up into atoms in a simple and unbiased way. Integration of local properties over atoms yields atomic properties. The gradient also determines the critical points, such as the BCP which characterizes a bond via the properties evaluated at it. This will be explained in more detail in the discussion below.

4. Computational details

All ab initio geometry optimizations were executed by the program GAUSSIAN94 [13] at the restricted Hartree–Fock (HF) level, BLYP level [14] second order

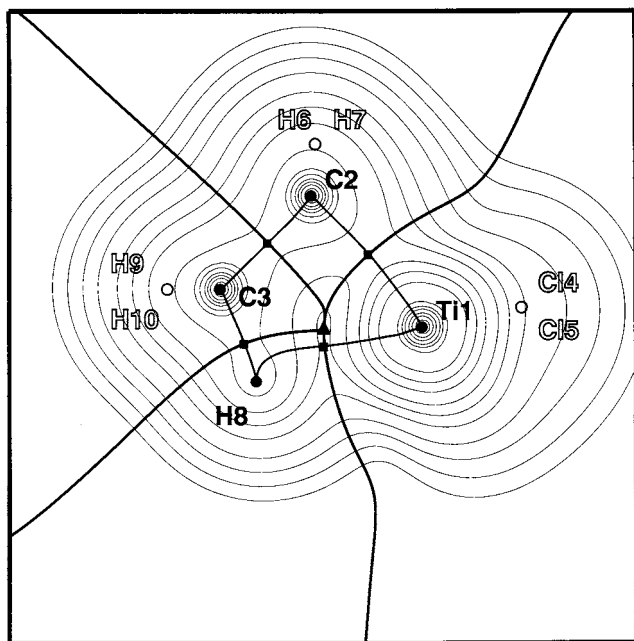


Fig. 2. Superposition of the contour lines (thin) of the charge density and the molecular graph (bold) and interatomic surfaces (bold) in the symmetry plane of $C_2H_5TiCl_2^+$ (**2**) (BLYP level). Bond critical points are denoted by squares and the ring critical point by a triangle. The labels of the nuclei that lie in the mirror plane are bold and those that do not lie in this plane are open. Note that the distance between the ring critical point and the agostic Ti–H bond critical point is very small. The bond path corresponding to the agostic interaction is quite curved near the agostic hydrogen atom H_8 .

Møller–Plesset perturbation theory (MP2) level using the MIDI4 basis set [15] for Ti and 6–31G** [16] for the other atoms (Cl, C and H). All stationary points are guaranteed to be minima via inspection of an analytical Hessian. The topological analysis was performed using the program MORPHY97 [17]. The positions of the critical points were detected using the eigenvector following method [18]. The charges of any molecule's atoms add up to maximum 0.003e and the sum of the atomic energies differs by maximum 1.6 kJ mol^{-1} from the total energy. These errors are acceptable within the context of the present study.

5. Results and discussion

5.1. Geometries and energies

Fig. 1 shows the six molecules that have been optimized. The corresponding energies and selected geometrical parameters are summarized in Tables 1–4. This set of molecules constitutes a staggered (**1a**) and an eclipsed (**1b**) conformation of $CH_3TiCl_2^+$, a single conformation of $C_2H_5TiCl_2^+$ (**2**) and three conformations of $C_3H_7TiCl_2^+$ (**3a–c**). In conformation **3a** there is a bond between Ti and C (as shown below) which is ruptured

and subsequently replaced by a Ti–H agostic bond (**3b**) upon rotation of the terminal methyl group along the $C_3–C_{10}$ bond. Finally we have included an open conformation (**3c**) in which no special Ti bond occurs. All molecules possess a mirror plane (C_s symmetry). Agreement with previously published geometries computed at a lower level [11,12] is good. All energies calculated via the BLYP method are consistently (and considerably) lower than those computed with MP2.

First we discuss the stability of the geometrical data with respect to the level of calculation (HF, BLYP, MP2). Correlation tends to lengthen all bonds except the agostic bonds Ti– H_8 (in **2**) and Ti– H_{12} (in **3b**) which become shorter by about 0.05 \AA . The BLYP method is inclined to lengthen the bonds in a more pronounced way than the MP2 ones except for Ti–Cl. Furthermore correlation quite dramatically decreases the Cl–Ti–Cl angle thereby allowing the Cl atoms to approach one another closer. The energy difference ΔE between conformers **1a** and **1b** is marginally affected by correlation: $\Delta E(\text{HF}) = 2.1 \text{ kJ mol}^{-1}$, $\Delta E(\text{BLYP}) = 2.7 \text{ kJ mol}^{-1}$ and $\Delta E(\text{MP2}) = 2.2 \text{ kJ mol}^{-1}$. However correlation inclusion has a more dramatic effect on the energy difference between a conformation possessing an agostic bond than one without it. Indeed, according to the HF calculation, conformer **3c** is 19 kJ mol^{-1} lower than **3b** whereas BLYP claims this difference to be only 3 kJ mol^{-1} .

Secondly we focus on trends and features which are qualitatively independent of the method of calculation. The Ti– H_{12} agostic bond is about 1.9 \AA and the Ti– H_8 agostic bond is slightly longer, 2.0 \AA , and therefore expected to be weaker. This hypothesis will be confirmed below by most AIM properties. Intuitively this observation appears plausible in view of the strain caused by the short alkyl chain in **2**. The long Ti– C_{10} bond unique to compound **3a** is about 2.2 \AA . The $C–H_{\text{agos}}$ bond which participates in the Ti–H–C system is exceptionally long, up to 1.14 \AA . Even the two other C–H bonds on the methyl group containing the agostic hydrogen show a consistent increase in bond length, up to 1.10 \AA . Also if the bond occurs between Ti and C as in Ti– C_{10} of **3a** the adjacent C–H bond length ($C_{10}–H_{11}$) increases to 1.12 \AA . This effect is more enunciated when this adjacent C–H bond is directed towards the Ti as it follows from the comparison between **3a** and **3b**. This observation triggers in turn the conjecture that the proximity of Ti tends to lengthen a close by C–H bond. This is confirmed by comparing the C–H bond lengths appearing in **1a** and **1b**. Even the C– H_9 bond in **3c** which is also directed to the Ti is longer than the more remote $C_{10}–H_{12}$. Inspection of certain valence angles reinterprets this bond lengthening effect as titanium's capability to draw a vicinal hydrogen closer to itself. This is clearly illustrated by the considerable decrease in the Ti–C– H_3 angle in going

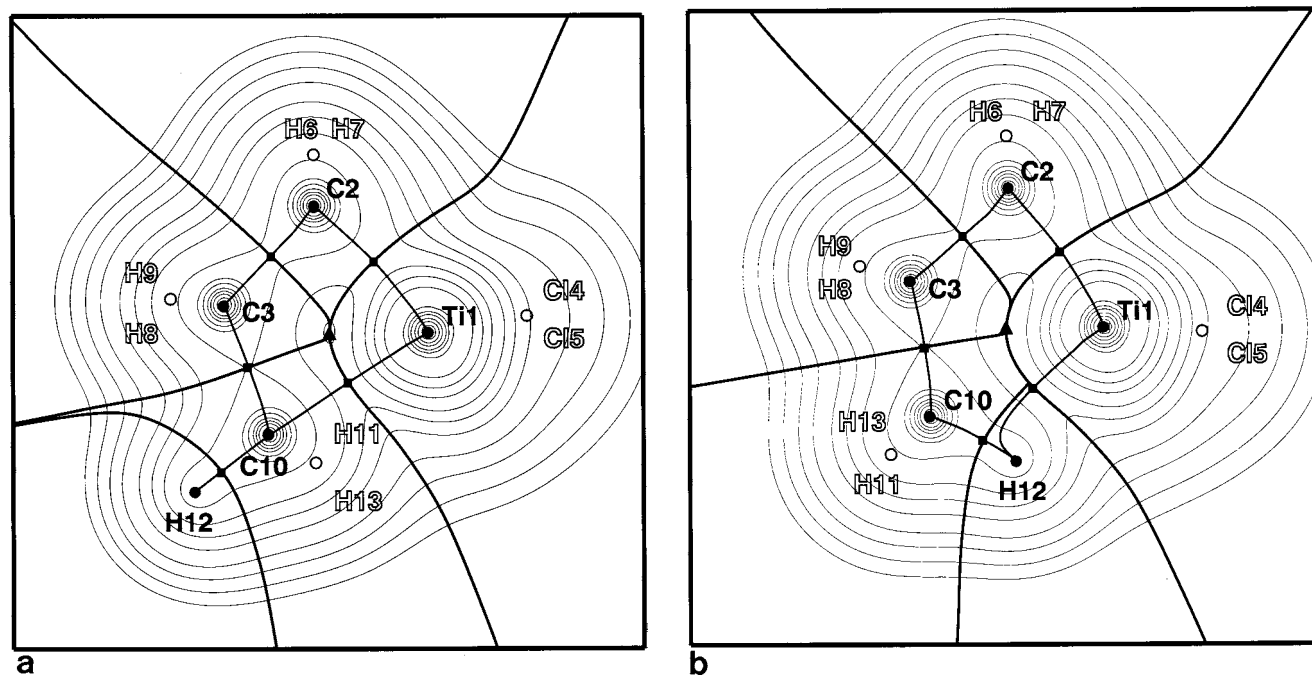


Fig. 3. Superposition of the charge density, the molecular graph and the interatomic surfaces in the symmetry plane of $C_3H_7TiCl_2^+$ (**3a**) (top) and $C_3H_7TiCl_2^+$ (**3b**) (bottom). The same conventions apply as in Fig. 2. This diagram (comparing top and bottom) illustrates the change in structure occurring when the C_{10} methyl group is rotated around the C_2-C_3 bond. In **3a** Ti is bonded to C_{10} which consequently becomes hypervalent (five atoms are bonded to it) but in **3b** Ti is bonded to the agostic hydrogen H_{12} . Note that the agostic bond path connecting Ti and the agostic hydrogen H_{12} is very curved near the latter atom.

from **1a** to **1b**. It should be pointed out that Ti has this 'pulling' capability even towards a hydrogen attached to a carbon, notably in the absence of an agostic bond. Finally the terminal methyl group of the open conformation **3c** is virtually an unperturbed sp^3 carbon.

5.2. Criteria based on the charge density

In this section we discuss a set of AIM features of agostic bonds as they occur in Ti-alkyl compounds.

5.2.1. Topology

Figs. 2 and 3b show the topology of the charge density in the symmetry plane of molecules **2** and **3b** which both contain an agostic bond. The existence of an agostic bond is clearly proven by the following triplet of concomitant topological objects: a BCP, a BP and an interatomic surface (IAS). The latter is a bundle of gradient paths originating at infinity and terminating at the BCP. This surface forms the boundary between two atoms sharing a BCP, hence its name. The BCP roughly lies in the middle of the bond path which is quite curved near the agostic hydrogen.

Inside the four membered ring (Ti-H-C-C) there is a ring critical point (RCP) which is the other kind of 'saddle'-type critical point conjugate to the BCP. In the RCP the charge density is a maximum with respect to one direction and a minimum with respect to the two

remaining perpendicular directions. Close proximity of the RCP to the BCP indicates structural instability. In other words the RCP and BCP may coalesce and annihilate each other in response to a small perturbation of the molecule's geometry. The ease with which the agostic bond can be ruptured via this mechanism is related to the previously stated conjecture that this is a weaker bond.

5.2.2. The electron density of the bond critical point

This quantity is denoted by ρ_b and is listed in Table 5 for compounds **1a** and **1b**, in Table 6 for **2** and in Table 7 for **3a**, **b** and **c**. It amounts to about 0.04–0.05 a.u.. A relation between ρ_b and the bond order and thus the bond strength has been exposed before [19]. On these grounds we expect the value for ρ_b of an agostic bond to be much lower than that of a typically covalent bond such as C-H. Again we can use this quantity to confirm that Ti-H₈ (in **2**) is a weaker bond than Ti-H₁₂ (in **3b**), a conclusion which holds at any level of computation (see Tables 5 and 7). Secondly the ρ_b value lies outside the interval 0.002–0.035 a.u. previously proposed to characterize hydrogen bonds [20].

Diagonalization of the Hessian of the charge density $\nabla\nabla\rho$ yields three (ordered) eigenvalues $\lambda_1 < \lambda_2 < \lambda_3$. The ellipticity ε is defined as $(\lambda_1/\lambda_2) - 1$ and measures the extent to which charge is preferentially accumulated. For example, the C-C bond shows an increasing ellip-

Table 5
Analysis^a of the bond critical points (BCP) in CH₃TiCl₂⁺ (**1a**) and (**1b**)

| | | HF (1a) | BLYP (1a) | MP2 (1a) | HF (1b) | BLYP (1b) | MP2 (1b) |
|------------------|------------------|------------------|--------------------|-------------------|------------------|--------------------|-------------------|
| Ti–C | ρ_b | 0.1430 | 0.1343 | 0.1353 | 0.1459 | 0.1327 | 0.1329 |
| | $\nabla^2\rho_b$ | –0.0476 | 0.0180 | 0.1012 | –0.0703 | 0.0230 | 0.1003 |
| | ε | 0.0226 | 0.0237 | 0.0321 | 0.0006 | 0.0001 | 0.0035 |
| Ti–Cl | ρ_b | 0.1140 | 0.1073 | 0.1114 | 0.1109 | 0.1074 | 0.1114 |
| | $\nabla^2\rho_b$ | 0.3442 | 0.3210 | 0.3695 | 0.3469 | 0.3210 | 0.3700 |
| | ε | 0.1015 | 0.0734 | 0.0623 | 0.1025 | 0.0672 | 0.0551 |
| C–H ₃ | ρ_b | 0.2878 | 0.2694 | 0.2769 | 0.2703 | 0.2484 | 0.2498 |
| | $\nabla^2\rho_b$ | –1.1547 | –0.9357 | –1.0099 | –0.9442 | –0.7376 | –0.7517 |
| | ε | 0.0007 | 0.0222 | 0.0279 | 0.0135 | 0.0357 | 0.0541 |
| C–H ₄ | ρ_b | 0.2718 | 0.2589 | 0.2605 | 0.2893 | 0.2697 | 0.2747 |
| | $\nabla^2\rho_b$ | –0.9647 | –0.8282 | –0.8435 | –1.1411 | –0.9300 | –0.9784 |
| | ε | 0.0243 | 0.0365 | 0.0519 | 0.0163 | 0.0283 | 0.0373 |

^a Symbols are explained in the text.

ticity in going from ethane over benzene to ethene. Not only does the ellipticity provide a measure for the π character of a bond but also its structural stability. The substantial bond ellipticities found for the agostic bonds reflect their structural instability [21] but a comparison between the actual magnitudes of the two bonds' ellipticity wrongly predicts that Ti–H₁₂ would be structurally the least stable.

5.2.3. The laplacian of the electron density of the bond critical point

The Laplacian $\nabla^2\rho_b$ is simply the sum of the eigenvalues λ_i . It has been observed that for ionic bonds, hydrogen bonds and van der Waals interactions (so-called closed-shell interactions) $\nabla^2\rho_b$ is positive. For

Table 6
Analysis of the bond critical points (BCP) in C₂H₅TiCl₂⁺ (**2**)

| | | HF | BLYP | MP2 |
|---------------------------------|------------------|---------|---------|---------|
| Ti–C | ρ_b | 0.1341 | 0.1249 | 0.1270 |
| | $\nabla^2\rho_b$ | –0.0445 | 0.0272 | 0.0962 |
| | ε | 0.0103 | 0.0301 | 0.0219 |
| Ti–Cl | ρ_b | 0.1118 | 0.1054 | 0.1107 |
| | $\nabla^2\rho_b$ | 0.3554 | 0.3192 | 0.3648 |
| | ε | 0.1177 | 0.0809 | 0.0711 |
| C ₂ –C ₃ | ρ_b | 0.2453 | 0.2330 | 0.2322 |
| | $\nabla^2\rho_b$ | –0.5968 | –0.4676 | –0.4808 |
| | ε | 0.0547 | 1.1727 | 0.1011 |
| C ₃ –H ₈ | ρ_b | 0.2460 | 0.2348 | 0.2433 |
| | $\nabla^2\rho_b$ | –0.7365 | –0.6172 | –0.6853 |
| | ε | 0.0176 | 0.0089 | 0.0101 |
| Ti–H ₈ | ρ_b | 0.0402 | 0.0381 | 0.0410 |
| | $\nabla^2\rho_b$ | 0.1761 | 0.1474 | 0.1815 |
| | ε | 0.7034 | 1.1727 | 1.9245 |
| C ₂ –H ₇ | ρ_b | 0.2898 | 0.2728 | 0.2778 |
| | $\nabla^2\rho_b$ | –1.1372 | –0.9397 | –0.9898 |
| | ε | 0.0194 | 0.0374 | 0.0501 |
| C ₃ –H ₁₀ | ρ_b | 0.2915 | 0.2764 | 0.2850 |
| | $\nabla^2\rho_b$ | –1.1447 | –0.9797 | –1.0664 |
| | ε | 0.0023 | 0.0003 | 0.0030 |

covalent bonds (shared interactions) the Laplacian is negative.

That all C–H and C–C bonds are covalent is readily recovered from the respective tables. The Ti–Cl bond shows a combination of relatively low ρ_b values and a positive Laplacian at the BCP, both indicative of an ionic bond. The regular (shorter) Ti–C bonds such as Ti–C₂ in all six molecules invariably have a near zero ellipticity and $\nabla^2\rho_b$ value while ρ_b is moderately high. This is a unique 'bond fingerprint' not encountered in typical bonds of purely organic molecules. The Ti–C₁₀ bond of **3a** falls somewhat outside this set of typical Ti–C bonds because its ellipticity is considerable higher and ρ_b hovers near zero. These features-combined with its ca. 0.2 Å longer bond length-point towards a weaker, more fragile bond. This conclusion is compatible with its role in the dynamic bond formation and rupture of the Ti–H₁₂ agostic bond upon methyl rotation as discussed below.

Finally the agostic bond itself is characterized by a $\nabla^2\rho_b$ value ranging from 0.15 to 0.25 a.u.. Again this lies outside the interval that characterizes hydrogen bonds [20]. More violations of these criteria will be encountered below.

5.2.4. Net charge

All integrated properties can be found in Table 8 for **1a** and **1b**, Table 9 for **2** and Table 10 for (**3a**, **b** and **c**) and are calculated at BLYP level. Here we focus on the net charge on an atom $q(\Omega)$ which is given by the sum of the (positive) nuclear charge and the (negative) electronic charge associated with an atom. For example, if the atomic basin of chlorine contains 17.33 electrons then its net charge is –0.33 e.

The agostic hydrogen is slightly negative (–0.08 and –0.06e resp. in **2** and **3b**). To check the stability of such a value compound **2** was re-optimized and H₈ re-integrated using an extensive basis set for C, Cl and H denoted by 6–311G+(3df,2p). The net charge on

Table 7
Analysis of the bond critical points (BCP) in C₃H₇TiCl₂⁺ (**3a**), (**3b**) and (**3c**)

| | HF (3a) | BLYP (3a) | MP2 (3a) | HF (3b) | BLYP (3b) | MP2 (3b) | HF (3c) | BLYP (3b) | MP2 (3c) |
|----------------------------------|------------------|--------------------|-------------------|------------------|--------------------|-------------------|------------------|--------------------|-------------------|
| Ti–C ₁₀ | ρ_b | 0.0464 | 0.0536 | 0.0538 | — | — | — | — | — |
| | $\nabla_2\rho_b$ | 0.1946 | 0.1994 | 0.2218 | — | — | — | — | — |
| | ε | 0.3095 | 0.1575 | 0.1231 | — | — | — | — | — |
| Ti–H ₁₂ | ρ_b | — | — | — | 0.0442 | 0.0530 | 0.0509 | — | — |
| | $\nabla_2\rho_b$ | — | — | — | 0.2133 | 0.2376 | 0.2476 | — | — |
| | ε | — | — | — | 1.5336 | 2.7403 | 2.6066 | — | — |
| Ti–C ₂ | ρ_b | 0.1444 | 0.1276 | 0.1280 | 0.1493 | 0.1328 | 0.1301 | 0.1299 | 0.1275 |
| | $\nabla_2\rho_b$ | –0.0669 | 0.0452 | 0.1156 | –0.0453 | 0.0772 | 0.1384 | –0.0648 | 0.1249 |
| | ε | 0.0043 | 0.0148 | 0.0181 | 0.0193 | 0.0468 | 0.0442 | 0.0234 | 0.0595 |
| Ti–Cl ₄ | ρ_b | 0.1036 | 0.1035 | 0.1086 | 0.1040 | 0.1113 | 0.1085 | 0.1036 | 0.1094 |
| | $\nabla_2\rho_b$ | 0.3305 | 0.3116 | 0.3563 | 0.3384 | 0.3429 | 0.3606 | 0.3342 | 0.3446 |
| | ε | 0.1425 | 0.0713 | 0.0658 | 0.1314 | 0.0589 | 0.0556 | 0.1551 | 0.0767 |
| C ₂ –C ₃ | ρ_b | 0.2425 | 0.2194 | 0.2207 | 0.2333 | 0.2094 | 0.2085 | 0.2527 | 0.2239 |
| | $\nabla_2\rho_b$ | –0.5879 | –0.4096 | –0.4279 | –0.5376 | –0.3646 | –0.3728 | –0.6298 | –0.4231 |
| | ε | 0.0409 | 0.0824 | 0.0985 | 0.0476 | 0.0883 | 0.1054 | 0.0910 | 0.1118 |
| C ₃ –C ₁₀ | ρ_b | 0.2180 | 0.2017 | 0.2128 | 0.2045 | 0.2017 | 0.2023 | 0.2275 | 0.2834 |
| | $\nabla_2\rho_b$ | –0.4847 | –0.3519 | –0.4114 | –0.4267 | –0.3494 | –0.3691 | –0.5598 | –1.0072 |
| | ε | 0.0292 | 0.0364 | 0.0364 | 0.0073 | 0.0173 | 0.0127 | 0.0003 | 0.0175 |
| C ₂ –H ₆ | ρ_b | 0.2934 | 0.2727 | 0.2772 | 0.2935 | 0.2794 | 0.2781 | 0.2953 | 0.2791 |
| | $\nabla_2\rho_b$ | –1.1573 | –0.9359 | –0.9831 | –1.1614 | –0.9885 | –0.9943 | –1.1809 | –0.9843 |
| | ε | 0.0238 | 0.0405 | 0.0528 | 0.0299 | 0.0431 | 0.0571 | 0.0171 | 0.0317 |
| C ₃ –H ₈ | ρ_b | 0.2979 | 0.2789 | 0.2867 | 0.2992 | 0.2870 | 0.2882 | 0.2775 | 0.2654 |
| | $\nabla_2\rho_b$ | –1.1765 | –0.9828 | –1.0650 | –1.1902 | –1.0449 | –1.0798 | –0.9787 | –0.8413 |
| | ε | 0.0030 | 0.0031 | 0.0036 | 0.0053 | 0.0078 | 0.0098 | 0.0495 | 0.0398 |
| C ₁₀ –H ₁₁ | ρ_b | 0.2758 | 0.2587 | 0.2665 | 0.2971 | 0.2848 | 0.2860 | 0.2951 | 0.2834 |
| | $\nabla_2\rho_b$ | –0.9663 | –0.8048 | –0.8759 | –1.1889 | –1.0426 | –1.0772 | –1.1425 | –1.0072 |
| | ε | 0.0579 | 0.0488 | 0.0514 | 0.0186 | 0.0150 | 0.0154 | 0.0261 | 0.0175 |
| C ₁₀ –H ₁₂ | ρ_b | 0.2921 | 0.2734 | 0.2818 | 0.2564 | 0.2456 | 0.2463 | 0.2951 | 0.2824 |
| | $\nabla_2\rho_b$ | –1.1659 | –0.9706 | –1.0612 | –0.8057 | –0.6770 | –0.7005 | –1.1425 | –1.0029 |
| | ε | 0.0102 | 0.0083 | 0.0080 | 0.0290 | 0.0096 | 0.0150 | 0.0247 | 0.0166 |

the agostic hydrogen is then found to be -0.10 e. If we want to screen the agostic bond via the previously proposed criteria for hydrogen bonding [21] an important question is how the net charge of a nitrogen changes when it becomes part of an agostic bond. The atom H₁₂ in **3a** bears a slight positive charge and becomes negative in **3b** as part of the agostic bond. This is exactly the opposite of what is happening in hydrogen bond formation and is the third violation of the hydrogen bond criteria.

From inspection of the tables it is obvious that most positive charge resides on the Ti atom. Not only is the overall positive $+1$ located on Ti but this atom is further depleted of electronic charge by another $0.6e$. As expected the chlorine atoms are negative (ca. -0.3 e) and so are the carbon atoms bonded to the Ti (also ca. -0.3 e) except for C₁₀ (in **3a**) which is allocated about half this excess charge (-0.16 e). The other carbons atoms are marginally negative (minimum value -0.1 e) while all non-agostic hydrogen atoms are slightly positive (up to 0.14 e). The absence of any considerable charge transfer between C and H remote from the Ti is explained by the negligible difference in electronegativity between these two elements.

5.2.5. Atomic energy

The energy of the agostic hydrogen (Tables 9 and 10) is markedly lower than of the other (non-agostic) hydrogen atoms, by approximately 150 kJ mol⁻¹. This effect is again diametrically opposed to a hydrogen bond criterion requiring that the protic hydrogen atom be destabilized, i.e. its energy should rise. It appears that the magnitude of stabilization of a hydrogen participating in an agostic bond matches the magnitude of destabilization of a hydrogen participating in a hydrogen bond. The improved computation with the large diffuse basis set alters the stabilization energy by only 12%.

It is tempting to brand the agostic bond in **3b** as the stronger one because the stabilization of H₁₂ is slightly more pronounced. Of course this hypothesis rests on the assumption that a stronger bond perturbs the partaking atoms more than a weaker one.

5.2.6. The dipolar polarization

This value is 15–30% larger for an agostic hydrogen compared to a normal hydrogen. Again this phenomenon infringes the hydrogen bonding criterion which prescribes a decrease of this value. The proximity of the Ti shifts the electron cloud around the agostic

Table 8
Atomic properties (in a.u.) for atoms in $\text{CH}_3\text{TiCl}_2^+$ (**1a**) and (**1b**) calculated at BLYP level

| Atom | 1a | 1a | 1a | 1a | 1b | 1b | 1b | 1b |
|----------------|---------------|---------------|---------------|----------------|---------------|---------------|---------------|----------------|
| | q(Ω) | M(Ω) | v(Ω) | –E(Ω) | q(Ω) | M(Ω) | v(Ω) | –E(Ω) |
| Ti | 1.6197 | 0.190 | 104.8 | 849.2833 | 1.6252 | 0.182 | 104.1 | 849.2809 |
| C | –0.3648 | 0.443 | 95.2 | 37.8972 | –0.3574 | 0.455 | 95.9 | 37.8933 |
| H ₃ | 0.1228 | 0.106 | 42.5 | 0.5623 | 0.0346 | 0.131 | 49.5 | 0.5880 |
| H ₄ | 0.0722 | 0.120 | 46.6 | 0.5780 | 0.1114 | 0.109 | 43.3 | 0.5682 |
| Cl | –0.2607 | 0.388 | 224.5 | 460.2123 | –0.2615 | 0.388 | 224.7 | 460.2057 |
| Σ | 1.0007 | — | — | 1809.31081 | 1.0022 | — | — | 1809.31007 |
| E ^a | — | — | — | 1809.31079 | — | — | — | 1809.30978 |

^a This is the (original) total energy of the molecule associated with the analyzed wavefunction.

hydrogen further away from the nucleus, although this effect is stronger in molecule **2**.

5.2.7. Atomic volume

There is some evidence that the agostic hydrogen is larger than its non-agostic counterparts but this swelling is not dramatic although it amounts up to 15% in compound **2**. As before this observation transgresses the corresponding hydrogen bond criterion.

5.3. Summary of features

It is instructive to briefly summarize the features collected in this study that characterize the agostic bond and agostic hydrogen atom (Table 11). It is remarkable that all these features systematically violate the hydrogen bond criteria except the first one which establishes the presence of a bond topologically.

The conclusion that an agostic bond is not a special case of a hydrogen bond is independently confirmed by Braga and Desiraju and co-workers [22]. In their recent study on agostic interactions using the Cambridge Structural Database they quite rightly state that “...the nature of the agostic interaction, C–M, which involves an electron-rich species (the C–H bond) and an electron-deficient species (the M atom) is quite different from that of a hydrogen bond...”. It should be noted that this electron transfer picture is also confirmed via the net AIM charges.

Table 9
Atomic properties (in a.u.) for atoms in $\text{C}_2\text{H}_5\text{TiCl}_2^+$ (**2**) at BLYP level

| Atom | q(Ω) | M(Ω) | v(Ω) | –E(Ω) |
|----------------|---------------|---------------|---------------|----------------|
| Ti | 1.6067 | 0.148 | 96.0 | 849.4839 |
| C ₂ | –0.2805 | 0.433 | 83.0 | 37.8860 |
| C ₃ | –0.0264 | 0.079 | 71.4 | 37.7463 |
| Cl | –0.3031 | 0.373 | 228.2 | 460.2689 |
| H ₆ | 0.0945 | 0.111 | 43.6 | 0.5810 |
| H ₈ | –0.0809 | 0.155 | 50.3 | 0.6445 |
| H ₉ | 0.1003 | 0.113 | 43.3 | 0.5792 |
| Σ | 1.0024 | — | — | 1848.61891 |
| E | — | — | — | 1848.61844 |

Fig. 4 shows the shape of an agostic hydrogen in $\text{C}_3\text{H}_7\text{TiCl}_2^+$ (**3b**) extended to 10^{-6} a.u. charge density envelope. The practical atomic subspace is bounded by two interatomic surfaces and the constant density envelope.

6. Changes induced by rotation of methyl groups

In this section a few remarks are gathered on the effect of the rotation of the terminal methyl group in compounds **1** and **3**. Rotation along the C–Ti axis of the virtually neutral methyl group in **1a** shows which effect the Ti has on a vicinal hydrogen atom. In going from the staggered to the eclipsed conformation the C–H₃ bond becomes longer, the Ti–C–H₃ angle reduces to almost 90°, the ρ_b value is reduced and the electron population of H₃ increases. These effects are collectively reminiscent of the formation of an agostic bond (potentially between Ti and H₃) although there is clearly no BCP present. So although both geometrical effects and AIM properties point in the direction of α -agostic interaction we do not find a bond expressing this interaction.

Agostic interactions with α hydrogens have been reported before in the literature. For example, experimental evidence for an α -agostic interaction has recently been presented by Etienne [23] in an Nb complex but the author did not prove there was an agostic bond. Also Ziegler and co-workers have observed an α -agostic interaction in a Zr complex [24] based on changes in the Zr–C _{α} –H angle and the tilting of the whole methyl group involved. Via partial geometry optimizations they attempted to assess the energy change associated with this agostic interaction. Finally in a pioneering ab initio MD study of zirconocene-catalyzed ethene polymerization by Meier et al. [25] an α -H agostic interaction was believed to be established in the early stages of the insertion process.

In summary we see that local and integrated AIM properties (such as ρ_b and the H population) predict

Table 10

Atomic properties (in a.u.) for atoms in $C_3H_7TiCl_2^+$ (**3a**), (**3b**) and (**3c**) at BLYP level

| Atom | 3a | | | | 3b | | | | 3c | | | |
|-----------------|---------------|---------------|---------------|----------------|---------------|---------------|---------------|----------------|---------------|---------------|---------------|----------------|
| | q(Ω) | M(Ω) | v(Ω) | -E(Ω) | q(Ω) | M(Ω) | v(Ω) | -E(Ω) | q(Ω) | M(Ω) | v(Ω) | -E(Ω) |
| Ti | 1.6117 | 0.155 | 85.5 | 849.6753 | 1.6081 | 0.136 | 81.5 | 849.6437 | 1.6088 | 0.160 | 94.0 | 849.6457 |
| C ₂ | -0.3042 | 0.450 | 84.2 | 37.8993 | -0.2906 | 0.503 | 84.3 | 37.9112 | -0.2759 | 0.461 | 82.6 | 37.8980 |
| C ₃ | -0.0079 | 0.065 | 63.0 | 37.7301 | -0.0517 | 0.066 | 62.9 | 37.7763 | -0.0942 | 0.010 | 58.7 | 37.7953 |
| Cl | -0.3343 | 0.361 | 229.9 | 460.3310 | -0.3286 | 0.343 | 228.6 | 460.2799 | -0.3216 | 0.371 | 229.7 | 460.3347 |
| H ₆ | 0.0890 | 0.112 | 43.9 | 0.5836 | 0.0876 | 0.113 | 43.4 | 0.5901 | 0.0867 | 0.114 | 44.5 | 0.5837 |
| H ₈ | 0.0796 | 0.116 | 43.7 | 0.5955 | 0.0809 | 0.116 | 42.3 | 0.6041 | 0.0002 | 0.142 | 47.9 | 0.6191 |
| C ₁₀ | -0.1629 | 0.143 | 68.8 | 37.8330 | -0.0811 | 0.110 | 70.7 | 37.7987 | 0.0927 | 0.143 | 69.5 | 37.6936 |
| H ₁₁ | 0.0295 | 0.131 | 45.8 | 0.6016 | 0.0986 | 0.115 | 42.4 | 0.5882 | 0.0457 | 0.122 | 46.6 | 0.6028 |
| H ₁₂ | 0.1373 | 0.105 | 41.2 | 0.5625 | -0.0617 | -0.135 | 44.6 | 0.6584 | 0.0491 | 0.122 | 46.6 | 0.6014 |
| Σ | 1.0016 | — | — | 1887.92365 | 1.0000 | — | — | 1887.91290 | 1.0027 | — | — | 1887.91460 |
| E ^a | — | — | — | 1887.92336 | — | — | — | 1887.91230 | — | — | — | 1887.91440 |

^a This is the (original) total energy of the molecule associated with the analyzed wavefunction.

the presence of an agostic interaction even in the absence of an agostic bond. In this case AIM provides an independent supplement of observations reinforcing the conjecture of an agostic interaction based on geometrical deviations.

The second issue to be discussed concerns Fig. 3 where we contrast the topology of compound **3a** with **3b**. The making or breaking of an agostic bond corresponds to a change in structure because the molecular graph which is the collection of bond paths changes. The atoms C₁₀ and H₁₂ compete for the BP linked to Ti. As the terminal methyl group spins around the C₃-C₁₀ axis a 'flip-flop' situation arises in which the Ti is now bonded to the C and then to the agostic hydrogen. This is probably the reason why many experts think of an agostic interaction as a σ interaction with the C-H group [26]. This rapid rotation of the methyl is well-known from NMR ('fluxional behaviour') and has also been studied theoretically, with the main focus on energy barriers [27]. It is possible to examine this structure change in detail using AIM and catastrophe theory [28] but this calls for a separate study.

Table 11

Summary of features of an agostic bond and an agostic hydrogen atom

- | | |
|-----|--|
| [1] | Topological pattern indicating the presence of a bond: a BCP, IAS and BP for H...M |
| [2] | The electron density at the bond critical point: 0.04–0.05 a.u. |
| [3] | The Laplacian of the charge density at the bond critical point: range 0.15–0.25 a.u. |
| [4] | Increased electron population (slightly negative net charge) |
| [5] | Energetic stabilization (lower energy than normal) |
| [6] | Increase of dipolar polarization |
| [7] | Slight increase in atomic volume |

Finally it is worth mentioning that the atom C₁₀ is a five-coordinated carbon. This is not a controversial observation in view of the maturity of hypercarbon chemistry [29]. For instance a remarkably stable gold complex containing a pentacoordinated carbon was recently discovered [30].

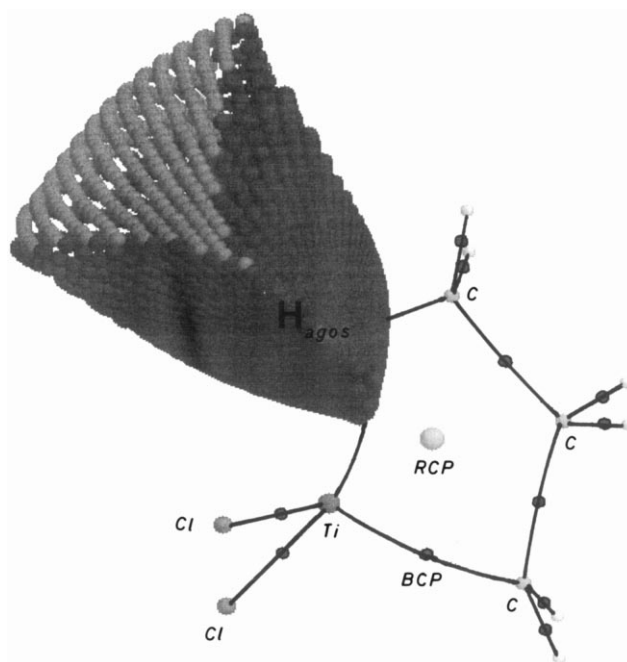


Fig. 4. A schematic diagram of the structure $C_3H_7TiCl_2^+$ (**3b**) showing the shape of the agostic hydrogen bounded by two interatomic surfaces and the $\rho = 10^{-6}$ a.u. envelope (set of medium dark spheres). The small light spheres represent the hydrogen atoms (unlabeled), the large light sphere is the ring critical point (RCP) and the small dark spheres are the bond critical points (one is labeled BCP). The agostic hydrogen atom H₁₂ is just marked symbolically, i.e. its real nuclear position is hidden inside the atomic basin.

7. Conclusion

It is possible to characterize a typical agostic bond with criteria purely based on the electron density. This technique is based on from the theory of AIM and is an independent complement to conventional methods like IR, NMR and structural crystallography. The observed features systematically violate the criteria that have been proposed for hydrogen bonding. As a consequence the agostic bond is not a special type of hydrogen bond. An agostic bond is not to be confused with hydrogen bonds such as the recently studied N–H...Co hydrogen bond for example [31]. It has been shown that AIM is a reliable tool in the characterization of the hydrogen bond [32]—even for extravagant ones such as the dihydrogen bond [33]. We have shown that AIM not only enables to prove the existence of an agostic bond but also reveals agostic interaction without the actual bond. It is hoped that the proposed tool will be used in conjunction with ab initio calculations in an attempt to guide experimental work [34] to further the understanding of metal catalyzed reaction pathways.

References

- [1] R.F.W. Bader, *Atoms in Molecules: A Quantum Theory*, Clarendon, Oxford, 1990.
- [2] R.F.W. Bader, P.L.A. Popelier, T.A. Keith, *Angew. Chem. Int. Ed. Engl.* 33 (1994) 620.
- [3] (a) S.J. LaPlaca, J.A. Ibers, *Inorg.Chem.* 4 (1965) 778. (b) N.A. Bailey, J.M. Jenkins, R.Mason, B.L. Shaw, *J. Chem. Soc. Chem. Commun.* (1965) 237.
- [4] S. Trofimenko, *J. Am. Chem. Soc.* 89 (1967) 6288.
- [5] S. Trofimenko, *J. Am. Chem. Soc.* 90 (1968) 4754.
- [6] F.A. Cotton, T. LaCour, A.G. Stanislawski, *J. Am. Chem. Soc.* 96 (1974) 754.
- [7] R.K. Brown, J.M. Williams, A.J. Schultz, G.D. Stucky, S.D. Ittel, R.L. Harlow, *J. Am. Chem. Soc.* 102 (1980) 981.
- [8] M. Brookhart, M.L.H. Green, *J. Organomet. Chem.* 250 (1983) 395.
- [9] C. Elschenbroich, A. Salzer, *Organometallics. A Concise Introduction*, VCH, Weinheim, 1992.
- [10] P. Roversi, M. Barzaghi, F. Merati, R. Destro, *Can. J. Chem.* 74 (1996) 1145.
- [11] H. Fujimoto, T. Yamasaki, H. Mizutani, N. Koga, *J. Chem. Soc.* 107 (1985) 6157.
- [12] H. Kawamura-Kuribayashi, N. Koga, K. Morokuma, *J. Am. Chem. Soc.* 114 (1992) 2359.
- [13] M.J. Frisch, G.W. Trucks, H.B. Schlegel, P. M. W. Gill, B.G. Johnson, M.A. Robb, J.R. Cheeseman, T. Keith, G.A. Petersson, J.A. Montgomery, K.Raghavachari, M.A. Al-Laham, V.G. Zakrzewski, J.V. Ortiz, J.B. Foresman, J. Cioslowski, B.B. Stefanov, A. Nanayakkara, M. Challacombe, C.Y. Peng, P.Y. Ayala, W. Chen, M.W. Wong, J.L. Andres, E.S. Replogle, R. Gomperts, R.L. Martin, D.J. Fox, J.S. Binkley, D.J. Defrees, J. Baker, J.P. Stewart, M. Head-Gordon, C. Gonzalez, J.A. Pople, *Gaussian 94*, Revision B.1, Gaussian, Inc., Pittsburgh PA, 1995.
- [14] (a) A.D. Becke, *Phys. Rev. A* 37 (1988) 785. (b) C. Lee, W. Yang, R.G. Parr, *Phys. Rev. B* 41 (1988) 785.
- [15] S. Huzinaga, J. Andzelm, M. Klobukowski, E. Radzio-Andzelm, Y. Sakai, H. Tatewaki, *Gaussian Basis Sets for Molecular Calculations*, Elsevier, Amsterdam, 1984.
- [16] R. Krishnan, J.S. Binkley, R. Seeger, J.A. Pople, *J. Chem. Phys.* 72 (1980) 650.
- [17] MORPHY97, a program written by P.L.A. Popelier with a contribution from R.G.A. Bone, UMIST, Manchester, UK, EU, 1997, UKIEU, 1997; P. Popelier, *Comp. Phys. Commun.* 108 (1998) 180.
- [18] P.L.A. Popelier, *Chem. Phys. Lett.* 228 (1994) 160.
- [19] K.B. Wiberg, R.F.W. Bader, C.D.H. Lau, *J. Am. Chem. Soc.* 109 (1987) 1001.
- [20] U. Koch, P. Popelier, *J. Phys. Chem.* 99 (1995) 9747.
- [21] D. Cremer, E. Kraka, T.S. Slee, R.F.W. Bader, C.D.H. Lau, T.T. Nguyen-Dang, P.J. MacDougall, *J. Am. Chem. Soc.* 105 (1983) 5069.
- [22] D. Braga, F. Grepioni, K. Biradha, G.R. Desiraju, *J. Chem. Soc. Dalton Trans.* (1996) 3925.
- [23] M. Etienne, *Organometallics* 13 (1994) 410.
- [24] T.K. Woo, L. Fan, T. Ziegler, *Organometallics* 13 (1994) 2252.
- [25] R.J. Meier, G.H.J. van Doremaele, S. Iarlori, F. Bu, *J. Am. Chem. Soc.* 116 (1994) 7274.
- [26] R.H. Crabtree, *Angew. Chem. Int. Ed. Engl.* 32 (1993) 789.
- [27] (a) Z. Lin, M.B. Hall, M.F. Guest, P. Sherwood, *J. Organometal. Chem.* 478 (1994) 197. (b) J.L.C. Thomas, M.B. Hall, *Organometallics* 16 (1997) 2318.
- [28] (a) R.F.W. Bader, T.T. Nguyen-Dang, Y. Tal, *Rep. Prog. Phys.* 44 (1981) 893. (b) J. Palis, S. Smale, *Pure Math.* 14 (1970) 223.
- [29] G.A. Olah, G. Rasul, *Acc. Chem. Res.* 30 (1997) 245.
- [30] H. Schmidbaur, F.P. Gabbai, A. Schier, J. Riede, *Organometallics* 14 (1995) 4969.
- [31] D. Zhao, F.T. Lapido, J. Braddock-Wilking, L. Brammer, P. Sherwood, *Organometallics* 15 (1996) 1441.
- [32] P.L.A. Popelier, *J. Phys. Chem.* 102 (1998) in press.
- [33] T.B. Richardson, S. de Gala, R.H. Crabtree, P.E.M. Siegbahn, *J. Am. Chem. Soc.* 117 (1995) 12875.
- [34] S. Zaric, M.B. Hall, *J. Phys. Chem. A* 101 (1997) 4646.